

NBSIR

JET DIFFUSION FLAME SUPPRESSION USING WATER SPRAYS  
An Interim Report

---

Center for Fire Research  
National Engineering Laboratory  
National Bureau of Standards  
Washington, D.C. 20234

Sponsored by:  
U.S. Department of Interior  
Minerals Management Service  
Reston, VA 22091

March 1983

---

U.S. DEPARTMENT OF COMMERCE

NATIONAL BUREAU OF STANDARDS

NBSIR

JET DIFFUSION FLAME SUPPRESSION USING WATER SPRAYS  
An Interim Report

---

B. J. McCaffrey

Center for Fire Research  
National Engineering Laboratory  
National Bureau of Standards  
Washington, D.C. 20234

March 1983

---

U.S. DEPARTMENT OF COMMERCE, Malcolm Baldrige, Secretary

NATIONAL BUREAU OF STANDARDS, Ernest Ambler, Director

# TABLE OF CONTENTS

|  | <u>Page</u> |
|--|-------------|
| List of Tables.....  | iv          |
| List of Figures.....   | iv          |
| Nomenclature.....  | v           |
| Abstract .....   | 1           |
| 1. INTRODUCTION.....   | 1           |
| 2. PREVIOUS OBSERVATIONS.....                                  | 4           |
| 2.1 Blowoff.....   | 5           |
| 2.2 Radiative Fraction.....                                    | 7           |
| 2.3 Dilution.....  | 8           |
| 2.4 Froude Number Regimes and Momentum.....                    | 9           |
| 2.5 Choked Flow.....   | 13          |
| 3. THEORY.....   | 15          |
| 3.1 Thermodynamic Equilibrium and Limit Flame Temperature..... | 15          |
| 3.2 Flame Stabilization.....                                   | 18          |
| 3.3 Momentum and Droplet Characterization.....                 | 21          |
| (a) Kalghatgi's Effect of Crosswind.....                       | 21          |
| (b) Droplet Dynamics.....                                      | 22          |
| (c) The Grand Model.....                                       | 24          |
| 4. EXPERIMENTAL RESULTS.....                                   | 25          |
| 4.1 Pneumatic Atomizing Nozzles.....                           | 25          |
| 4.2 Centerline Temperature.....                                | 26          |
| 4.3 Scaling the High Momentum Limit.....                       | 28          |
| 4.4 Effect of Spray.....                                       | 30          |
| 4.5 Equilibrium Heat of Reaction Calculation.....              | 32          |
| 4.6 Flame Temperature Measurements.....                        | 37          |
| 4.7 Correlation with Drop Size.....                            | 39          |
| 5. CONCLUSIONS AND RECOMMENDATIONS FOR FUTURE STUDY.....       | 41          |
| 6. REFERENCES.....   | 43          |

## LIST OF TABLES

|   | <u>Page</u> |
|---|-------------|
| Table 1. Scaling.....   | 1           |
| Table 2. Critical Diameters for Absolute Flame Stability..... | 14          |

## LIST OF FIGURES

|   | <u>Page</u> |
|---|-------------|
| Figure 1. "Extinguishment" by Water Spray.....  | 46          |
| Figure 2. Radiative Fraction Reduction Due to Water Spray or Other Additive.....      | 47          |
| Figure 3. Photographs of Spray-Suppressed Flames.....                                 | 48          |
| Figure 4. Radiative Fraction For Various Gases as a Function of Froude Number.....    | 49          |
| Figure 5. Sample Equilibrium Calculation and Effect of Water.....                     | 50          |
| Figure 6. Equilibrium Flame Temperature Reduction vs. Amount of Water.....            | 51          |
| Figure 7. First Stage (Momentum) of Droplet-Flame Interaction Model.....              | 52          |
| Figure 8. Pneumatic Atomizing Nozzle.....   | 53          |
| Figure 9. Hydrogen Flame Temperature Measurements.....                                | 54          |
| Figure 10. Correlated Temperature Measurements Without Water.....                     | 55          |
| Figure 11. Correlated Temperature Measurements With Water.....                        | 56          |
| Figure 12. Derived Heat Release Reduction vs. Amount of Water.....                    | 57          |
| Figure 13. Normalized Flame Temperature Reduction vs. Amount of Water.....            | 58          |
| Figure 14. Normalized Flame Temperature Reduction Correlated by Median Drop Size..... | 59          |

# NOMENCLATURE

|                   |  |
|-------------------|--|
| A,B               | experimental constants, Eq. (9)  |
| D                 | gas jet exit diameter  |
| $D_{CR}$          | critical diameter for absolute stability   |
| $D_P$             | droplet particle diameter  |
| $F_o$             | gas jet Froude Number = $U^2/gD$   |
| g                 | gravitational acceleration   |
| $H_f$             | flame height   |
| $\Delta H_f^o$    | heat of formation  |
| $\Delta H_{COMB}$ | heat of combustion, equilibrium calculation, Eq. (7)                                   |
| $\dot{m}_{gas}$   | mass flow rate of gas (fuel)   |
| $\dot{m}_{H_2O}$  | mass flow rate of water  |
| n                 | number of moles  |
| $\dot{n}$         | molar flow rates   |
| Q                 | nominal heat release rate or net calorific potential of fuel                           |
| $Q_E$             | equivalent heat release rate, $Q - Q_{H_2O}$   |
| $Q_{H_2O}$        | energy depleting potential of water, see Eq. (6)                                       |
| $Q_R$             | that fraction of Q which is radiated away from flame region                            |
| $t^*$             | dimensionless time, $tV_o/D_P$   |
| T                 | absolute temperature ( $T_o$ , ambient; $T_f$ , flame temperature)                     |
| $\Delta T$        | temperature difference referenced to ambient = $T - T_o$                               |
| $\Delta T_{D-W}$  | temperature difference without water referenced to with water =<br>$T_{DRY} - T_{WET}$ |
| U                 | gas jet exit velocity  |
| $V_g$             | gas jet velocity for droplet dynamics model  |
| $V_o$             | initial particle velocity  |
| $\bar{X}_m$       | median drop size, Eq. (10)   |

$x^*$  dimensionless horizontal coordinate,  $x/D_p$   
 $y^*$  dimensionless vertical coordinate,  $y/D_p$   
 $z$  vertical distance above nozzle exit  
 $\chi$  radiative fraction -  $Q_R/Q$   
 $\phi$  fuel to air ratio divided by the fuel to air ratio at  
stoichiometric (equivalence ratio)

JET DIFFUSION FLAME SUPPRESSION USING WATER SPRAYS -  
An Interim Report

B. J. McCaffrey

Abstract

The feasibility of using water sprays for the control of offshore oil/gas well blowout fires has been addressed. On consideration of the sheer scale of the problem, knowledge from a fundamental viewpoint is going to be required in order to extrapolate laboratory-sized flame studies up to full scale. Available data and appropriate literature concerned with the application of water sprays as a jet diffusion flame suppression/extinguishment agent have been reviewed. Small pneumatic atomizing nozzles using  $H_2$  gas, both as the flame source as well as the atomizing driver, have been used to scale high momentum jet flames and to study the effect of water on the flame. Thermodynamic equilibrium was shown to be an effective guide in interpreting the results. The effect of flame temperature reduction due to water sprays has been observed to correlate with a single spray parameter - the median drop diameter. Directions for further study have been indicated.

1. INTRODUCTION

The object of this work is to study the interaction of water droplet sprays with high momentum jet flames in order to elucidate the physio-chemical mechanisms responsible for flame suppression/extinguishment. The study will provide the basis for estimating the feasibility of using water sprays for off-shore oil/gas well blowout fire protection. Due to the sheer scale of the problem manifested in the large quantities of gas involved in blowout fires it will be impossible to extrapolate or scale upward, with any degree of

certainty, the results and conclusions of laboratory-scale experiments without this fundamental understanding of the participating mechanisms.

In the final analysis the feasibility of the concept will depend on whether the amount of water deemed necessary for suppression/extinguishment is within the pumping power of the off-shore facility. A tacit assumption prevailing here is the existence of a virtually limitless supply of water (and pumping power) as opposed to some stored chemical inhibitor which would perhaps provide a more effective suppression action initially but might prove to be deficient in the circumstances of re-ignitions or lack of total extinguishment. From engineering considerations of scale the variable chosen here to represent the amount of water is the ratio of the mass flow rate of water to that of the gas,  $\dot{m}_{H_2O}/\dot{m}_{gas}$ . The feasibility of the approach will depend strongly on how reasonable (as yet undefined) this ratio turns out to be.

The following table gives an estimate of the scale in terms of fire size attainable in various laboratories contrasted to the full scale expected blowout fire size.

Table 1. Scaling

|                          | <u>Fire Size</u> |                            |  |
|--------------------------|------------------|----------------------------|--|
|                          | <u>MW</u>        | <u>Mft<sup>3</sup>/day</u> | <u><math>\dot{m}_{H_2O}/\dot{m}_{gas}</math><br/>(for 5000 liters/min)</u> |
| Small Laboratory         | .01 - .1         |                            |  |
| Large Laboratory         | 1 - 10           | 0.1 - 1                    |  |
| Industrial Test Facility | 100              | 10                         | 50   |
| Full Scale Blowout       | 1000             | 100                        | 5  |

Also shown is the equivalent expected order of gas flow in millions of cubic feet per day. It is conceivable then to reach, with experiment, to within one order of magnitude of full scale. Information garnered at each lower scale where more detailed measurements can be made increases confidence in scaling to larger and larger fires.

The third column in the table shows the ratio of water to gas,  $\dot{m}_{H_2O}/\dot{m}_{gas}$ , if 5000 liters/min of water were available for fire fighting. That water flow rate was reported to be provided in cooling the equipment used to cap a recent blowout fire in South Yorkshire<sup>1</sup>. In terms of the full scale blowout a ratio in the order of 5 for flame extinguishment may prove to be reasonable.

Some of the nozzle-flame configurations discussed in this report involve spraying directly within the flame envelope. This direct injection allows most, if not all, of the spray to participate in the suppression process. Other situations involve an external spray in, perhaps, a more conventional fire fighting configuration, where the spray is directed at the flame from some lateral distance and angle. Unlike the internal spray, in certain situations not all of the spray will get involved in putting out the fire. However, once the physio-chemical mechanisms are identified and understood in terms of changes in measurable quantities (temperature, radiation, species concentration, etc.) due to the spray, a correspondence can be established between the more ideal internal spray configuration and any external configuration. It is proposed that changes in the observable effects between the two cases can be related to the effectiveness of physically bringing the

---

<sup>1</sup>Refer to reference location at end of text.

spray into the suppression process. (If in other situations it appears that momentum of the spray may be useful in separating the flame from a holder then the external configuration might be a more effective means to extinguishment.)

It is this basic understanding of which processes are operating in which circumstances that will ultimately lead to the engineering design data required for the determination of flow rates, placement of nozzles, etc.

## 2. PREVIOUS OBSERVATIONS

O'Neill<sup>2</sup> has studied the effect of external sprays on CH<sub>4</sub> diffusion flames emanating from a 25 mm ID pipe burner. He varied the nozzle type, transverse and lateral distances, and angle with respect to the vertical burner. Of the matrix of combinations attempted, it was determined that the flame could be extinguished by a 30° full cone spray nozzle located at an angle with respect to the horizontal of 50° or more, located near or below the burner exit at a short distance laterally. Extinguishment was accomplished with  $\dot{m}_{H_2O}/\dot{m}_{CH_4}$  ratios of less than 10.

As part of the initial feasibility work, additional experiments at smaller scale were performed using an internal spray configuration. The design chosen consisted of a spray nozzle located concentrically within a cylindrical pipe which supplied the gaseous fuel for the diffusion flame simulation. This design would allow most, if not all, of the water to reach, or otherwise be entrained into, the combustion region. The fuel pipe was a standard 25 mm ID (1") wrought iron pipe. The nozzle, contained in an 18.3 mm OD fitting, was a standard residential oil burner nozzle (Delavan 1.5 and 2.5-

30°B)\*, solid cone type with a nominal 30° spray angle, which protruded about 13 mm above the end of the fuel pipe. The gas, commercial propane, would flow through the annulus formed by the outside pipe and the inside nozzle fitting in a diffusion mode. Gas and water flows were monitored using standard flowmeters.

Figure 1 presents data from both O'Neill's<sup>2</sup> and the small scale internal configuration. The ordinate is a linear scale of the water to gas ratio at "extinguishment", the term used loosely at this point to indicate a flame is no longer present. Prior to their actual disappearance, these flames are effectively lifted-off and sometimes "exist" as a small ball of pale pinkish-yellow luminosity high above the burner exit at significantly lower water flow rates than those reported here for extinguishment. The abscissa is a log scale of nominal heat release rate of the fire, giving a graphical presentation of the scale of the problem as indicated in Table 1. The dots or points are actual data, the lines indicate faired trends of the data. The A, B, C follows O'Neill<sup>2</sup> size designation as does 2.5 and 1.5 follow the manufacturers designation for the internal spray. The ratios of the flow rate capacities of nozzle B:A:C are approximately 4:2:1. The small scale flow rate ratio for the two nozzles is 2.5:1.5. The lower series of "C" points are results for vertical upward spraying, the numbers are distances (in feet) between the spray nozzle exit and the burner exit elevation.

---

\*Implies no endorsement by NBS.

## 2.1 Blowoff

The trends of the data at both scales appear similar, the smaller scale having greater flexibility in gas flow rates. That is, as the heat release rate or gas flow rate or velocity increase, the relative amount of water reflected in  $\dot{m}_{H_2O}/\dot{m}_{gas}$  required for extinguishment decreases. What becomes immediately apparent if one extrapolates these results to higher and higher velocities and correspondingly smaller and smaller amounts of water is that the phenomenon of blowoff manifests itself. For a fixed burner size, as the gas velocity is increased further the flame begins to lift off of the burner. As velocity is further increased this lift-off distance, the distance between the burner and the base of visible luminosity of the flame increases until finally flame stabilization becomes impossible. This is without any water or other diluent. The gas flow velocity appears to exceed a burning velocity everywhere. Note the acetylene data from the pneumatic atomizing nozzle "PAN" (to be discussed later) on Fig. 1. The last point shows extinguishment with no water. This is more correctly blowoff rather than any conventional expression of extinguishment. Shown also on Fig. 1 are some results due to Kalghatgi<sup>3</sup> who has recently studied the blowout phenomenon of diffusion flames of pure gases and gases with diluents. On the figure are shown his results for a propane flame diluted with inert  $CO_2$  ( $\dot{m}_{CO_2}$  would obviously replace  $\dot{m}_{H_2O}$  for the ordinate). With no  $CO_2$  added the flame blows off at a certain velocity (converted to Q). As the amount of  $CO_2$  that is premixed into the propane increases, the exit velocity at blowoff decreases, not unlike both sets of present data shown on Fig. 1 utilizing water sprays. It might be

argued that spraying liquid water and premixing a diluent should yield different behavior due to different mechanisms operating but Fig. 1 alone does not, at this point, indicate significant differences.

## 2.2 Radiative Fraction

Additional insight into the behavior of the small scale concentric nozzle-burner configuration may be obtained from Fig. 2 which shows the decrease in the radiative fraction,  $\chi/\chi_0$ , with increased water to gas ratio. The radiative fraction is that portion of the total nominal heat release rate of the fire ( $Q$ ) which is radiated away ( $Q_R$ )

$$\chi = Q_R/Q \quad (1)$$

Representative values for common gases and experimental details are given in Ref. 4.  $\chi_0$  is the value of the radiative fraction for the flame without water addition. Three sets of data presented on Fig. 2 represent three water flow rates or more importantly three nozzle pressures. (These are simple  $\Delta p \sim V^2$  devices). As pressure increases the water becomes more effective in reducing radiation. It is well established that spray droplet size varies inversely with pressure and hence a tentative explanation for the better performance at higher pressures could involve smaller droplet size. In Fig. 2 the measurements were made with a constant water flow rate and a variable gas flow rate.

The vertical lines shown in Fig. 2 are the values of the water to gas ratio corresponding to extinguishment in the sense of Fig. 1. As well as

reduced radiation levels the higher pressure data appears to make extinguishment easier. Note the radiation reduction levels appear to reach a minimum (.4-.5) before extinguishment; they do not asymptotically go lower and lower perhaps indicating some flame stabilization mechanism is operating.

The series of photographs seen in Fig. 3 is what one observes as the amount of water is increased in going from left to right. (These results are for a pneumatic atomizing nozzle with nitrogen used as driver,  $\dot{m}_{N_2} / \dot{m}_{C_3H_8} = 0.4$ , the entire nozzle located concentrically within the pipe reducer seen in the pictures. They are, however, typical of all scales and all configurations noted in the present observations.) Most of the radiation in these diffusion flames is due to soot. The radiation reduction seen in Fig. 2 follows what the photographs indicate in Fig. 3. The bright yellow appearance changes to orange and becomes paler and paler as the water flow increases. In large-scale flares used in the chemical process industry, water in the form of steam (and other diluents) is often mixed with the effluent before burning, the purpose of which is to reduce the smoke and soot produced in the combustion process for environmental considerations<sup>5</sup>. Since soot is the dominant emitter it appears then that there is a strong correlation between the photographs in Fig. 3 and the reduced radiation seen in Fig. 2.

### 2.3 Dilution

Shown on Fig. 2 are some results from Gupta<sup>6</sup> in which the diluents, steam and argon, were mixed with the propane prior to burning. Similar behavior to the present sprays, especially the high pressure results, is observed. One can immediately begin to speculate about another mechanism, besides blowoff,

which may be operating here and that is dilution. If a diluent or non-participating gas is carried along with the fuel it must be heated in the process thereby extracting energy from the flame and resulting in a lower flame temperature than would result in its absence. Additionally the diluent could interfere with the burning by displacing some oxygen in the entrainment/mixing process resulting in a lowered overall combustion efficiency. For whatever reason the soot formation/oxidation process is being interfered with by either premixing or spraying in a diluent.

If plotted on a molar basis,  $\dot{n}_{\text{DILUENT}}/\dot{n}_{\text{C}_3\text{H}_8}$ , the striking difference between the argon and steam (and highest pressure spray results) data on Fig. 2 would disappear - the data would virtually fall on the same line. This is in spite of the fact that there is a factor of 2 to 2-1/2 times (depending on temperature) difference in heat capacity,  $C_p$ , between argon and steam. Judged on a purely flame temperature reduction the steam ought to be significantly more effective than argon. Complete understanding of the soot formation/destruction process is a formidable problem!

#### 2.4 Froude Number Regimes and Momentum

In a discussion involving flame stabilization, blowoff, reduced radiative fraction and flame momentum, a convenient parameter for classifying diffusion flames from pipes has been found to be the Froude number<sup>4</sup>,

$$F_o = U^2/gD \quad (2)$$

The square root of  $F_0$  will be used here for convenience in compressing the scales.  $U$  is the exit velocity from the pipe or burner of diameter,  $D$ .  $F_0$  is a measure of the relative strength of the momentum of the gas stream compared to its potential buoyancy. In Ref. 4 it was seen that all non-laminar diffusion flames from pipes could be conveniently classified into three groups or regimes. For low  $F_0$ , i.e.,  $U$  is low and  $D$  is large, buoyancy is dominating. This is the case of pool fires,  $L/D \rightarrow 0$ , where  $L$  is the flame height. In this regime flame height and the radiative fraction are functions of both  $U$  and  $D$ . For smaller  $D$  and larger  $U$ ,  $F_0$  rises into an interesting, intermediate regime where  $L$  becomes independent of  $D$  and  $\chi_0$  depends only on the fuel and not on either  $U$  or  $D$ . In this very large intermediate regime all flames appear similar and scaling becomes simple.

Finally as  $D$  is decreased and  $U$  increased further one arrives at the fully turbulent, very noisy, high momentum jet flame characteristic of the blowout fire. In this regime, as the flame begins to lift-off, the flame height remains constant (as a function of  $D$ ) and the radiative fraction decreases with increased  $U$  as more and more air is entrained or sucked into the gas jet. Like the buoyant regime, the simple scaling of the intermediate regime is lost in this full momentum regime.

Fig. 4 shows the behavior of the radiative fraction  $\chi_0$  plotted against  $\sqrt{F_0}$  in the intermediate and momentum regimes. On the left hand side of the figure is seen the constant  $\chi_0$  for  $C_3H_8$ , independent of flow and diameter. The results of Ref. 4 ( $D$ : 5-40 mm tubes) are somewhat higher than Markstein's<sup>8</sup> (12.7 mm nozzle) results and thought to be due to better mixing in the case of the nozzle's sharp exit velocity profile<sup>4</sup>. On the left, Becker's<sup>7</sup> values

of  $\chi_0$  for different gases in natural convection flames (ignoring the purely buoyant, pool fire regime) follow the same order with the C/H ratio of the fuel as given in Ref. 4.

Brzustowski's<sup>9</sup> result for  $C_3H_8$  (and  $CH_4$ ) in 5 mm tubes is typical of the decreasing  $\chi_0$  as velocity is increased and momentum begins to dominate. This result is virtually identical to that in Ref. 4 in which a similar sized pipe was used. At the low  $\sqrt{F_0}$  end of the dotted line the higher  $\chi_0$  values might be more typical of a laminar flame. Obviously a single diameter pipe can not span the entire  $\sqrt{F_0}$  regimes - at low enough flow rates the flames will become laminar. (All of the results discussed here are for non-laminar flames.) As velocity is increased,  $\chi_0$  falls and then appears to reach a lower limit after which a further increase in velocity causes blowoff. Shown by vertical dashed lines is the Kalghatgi<sup>3</sup> correlation results of blowoff for the  $C_3H_8$  and  $CH_4$  flames in 5 mm ducts. (Blowoff for a 2.1 mm duct burning  $C_3H_8$  from Ref. 4 shown by a solid vertical line compares favorably to the Kalghatgi<sup>3</sup> prediction.)  $\chi_0$  remains at about 0.15 until blowoff. This behavior of decreasing  $\chi_0$  to some limit, then blowoff, is reminiscent of the behavior of  $\chi/\chi_0$  seen in Fig. 2 where the signal decreased with water flow rate to some limit, with further water causing "extinguishment".

Shown further on into the momentum regime are small D, large U results for acetylene and hydrogen. The dashed lines are from Becker<sup>7</sup> for a 2.5 mm D tube, the data points are from a small annulus (to be discussed later). For very sooty acetylene  $\chi_0$  falls from quite a high value with increased velocity reaching a limit of about 5% followed by blowoff. Hydrogen with an even

higher burning velocity is stable to much higher  $F_0$  and as expected yields little radiation.

The value of a plot like Fig. 4 comes about in trying to sort out the various suppression mechanisms. Knowing where on the Froude number scale one is operating will help identify which processes are dominating. Recall that Fig. 1, which showed the ratios of water to gas for "extinguishment", contained an element of blowoff. On the other hand Fig. 2 showed what appears to be a real dilution effect. The larger scale O'Neill<sup>2</sup> data had  $\sqrt{F_0}$  ranging from 70 to 340, near the high momentum regime for 5 mm pipes but not necessarily for those of 25 mm. Recall that unlike the intermediate regime both U and D are needed to characterize the flame. Without measurements at this large size interpretation gets somewhat dubious. For the small annular results of Fig. 1 and 2, however, data exists and is shown as circles in Fig. 4 with  $\sqrt{F_0} = 1$  to 10. The radiative fraction for this annulus falls not unreasonably between the tube results of Ref. 4 and the nozzle results of Markstein<sup>8</sup> and appears to be removed from the blowoff end.

One sees now some confirmation of what appeared to be a real dilution effect in Figs. 2 and 3 - there is decreased radiation due to the water spray. Additionally, for large rates of water flow the 30° solid cone of spray can intersect the annular flowing gases and may contain sufficient momentum due to the droplets themselves as well as the accompanying entrained air so as to physically lift (or separate) the flame (or, at least, the visible portion) to such distance as to make flame stabilization impossible. This mechanism may be responsible for the "extinguishment" noted at high water flow rates. Elements of this may be present in the O'Neill<sup>2</sup> results as well. Prior to

lifting and "extinguishment", his descriptions of the changing color of the flame with water matches the small scale results.

Besides estimating blowoff in terms of dilution, e.g., the Kalghatgi<sup>3</sup> correlation coupled with thermodynamics, one also will require a model for relative momentum in terms of particle drop size in order to fully interpret the results of Fig. 2.

## 2.5 Choked Flow

There is another aspect to the blowout fire problem which could be extremely important and yet one for which combustion specialists are generally not aware of when dealing only with laboratory sized diffusion flames. The normal laboratory situation involves increasing the gas flow velocity,  $U$ , through a fixed diameter pipe,  $D$ , until the flame becomes lifted. Further increase in  $U$  causes the lift-off distance to increase until finally with further increase in  $U$  the flame blows off. Now, there is evidence that suggests that further increase in gas velocity (orders of magnitude in some cases) leads to a situation where a very stable supersonic flame can exist above the burner<sup>10</sup>. Furthermore there is a critical diameter,  $D_{CR}$ , above which flames are stable; that is, they cannot be blown off by increasing gas velocity. Annushkin and Sverdlov<sup>10</sup> present a model and some limited data for the boundary of flame instability, i.e., on a  $U$  (or pressure ratio) vs  $D$  plot, that area where blowoff can occur. The extreme of diameter, corresponding to flow velocities somewhat above Mach 1 for common gases, becomes the critical diameter, "above which absolute stability of the lifted flame is insured for any velocity"<sup>10</sup>.

The following table contains the estimate of critical diameter given in Ref. 10 and also those calculated by Kalghatgi<sup>3</sup> in extrapolating his small diameter correlation results.

Table 2. Critical Diameters for Absolute Flame Stability

| <u>GAS</u>                    | <u>D<sub>CR</sub>(mm)</u>                    |                              |
|-------------------------------|--|------------------------------|
|                               | <u>Annushkin &amp; Sverdlov<sup>10</sup></u> | <u>Kalghatgi<sup>3</sup></u> |
| H <sub>2</sub>                | 1  | --                           |
| C <sub>2</sub> H <sub>2</sub> | --   | 1.57                         |
| C <sub>2</sub> H <sub>4</sub> | --   | 14.5                         |
| C <sub>3</sub> H <sub>8</sub> | 6*   | 17.2                         |
| CH <sub>4</sub>               | 23   | 41.4                         |

\*Kalghatgi<sup>3</sup> (Part II) obtains blowoff for tubes of 6 and 8 mm diameter with zero crosswind.

Like most of these stability analyses the ordering of gases follows flame speed or burning velocity. Results can be calculated for other gases and mixtures using a host of thermophysical and transport properties. Ref. 10 contains data only for H<sub>2</sub> since the amount of other gases required is generally prohibitive. However, Kalghatgi<sup>3</sup> quotes some anecdotal evidence in which a stable flame existed on top of a 100 mm D pipe connected to a natural gas reservoir at a pressure of 85 atmospheres. Assuming isentropic flow and expanding from a stagnation pressure of 85 atm to atmospheric leads to an exit

Mach number of about 3.5 with a heat release rate in the order of 700 MW which would certainly qualify as a full scale blowout fire.

One must therefore be aware of the possibilities of choked flow in contemplating various extinguishment scenarios. The deviation between the two sets of results for critical diameter noted in Table 2 may be narrowed somewhat by experiments in later phases of this project. For the case of  $\text{CH}_4$  or natural gas, pipe sizes greater than 41 mm could be anticipated in the blowout situation, although not guaranteed since the actual rupture could occur in a number of places of smaller vent size throughout the labyrinth of piping on the rig. The mechanisms of suppression however, will be similar whether or not the flow is supersonic - on a molecular level the same chemistry will be operative. The physics could be somewhat different in terms of the pressure field around the exit, especially if a spray momentum mechanism was favored for extinguishment. If it turns out to be an important factor there are schemes available used for the study of supersonic rocket exhaust plumes which may be utilized to characterize this feature, see for example Ref. 11.

### 3. THEORY

Tools that are available for the quantification of some of the mechanisms alluded to in the previous section will be discussed in more detail in the following.

### 3.1 THERMODYNAMIC EQUILIBRIUM and Limit Flame Temperature

If a system not in chemical equilibrium, e.g., a mixture of  $H_2$  and air at room temperature, is allowed to approach equilibrium adiabatically the heat evolved from the chemical reaction will be used to raise the temperature of the products to what is called the adiabatic flame temperature. In other words, if the heat of combustion of the mixture is converted exclusively into thermal energy of the products the resulting temperature is called the adiabatic flame temperature. The state associated with this temperature, thermodynamic equilibrium, implies thermal, mechanical, and chemical equilibrium and the difference between it and the initial state represents the ideal energy potential of the reactants. Through thermochemical tables, charts or computer programs, the ideal energy potential is readily calculable knowing the initial temperature and amount of reactants. The output of the calculation includes the flame temperature and mole fractions of products.

Since no real flame can be completely adiabatic the adiabatic flame temperature represents an upper limit for actual temperature although certain premixed flames can exhibit temperatures close to those calculated. In general, diffusion flames will mirror or reflect equilibrium to some degree since equilibrium can be viewed as a flame with infinitely fast reaction rates taking place in an infinitesimal volume with no radiation. How the real flame differs regarding reaction rate and flame volume will determine how well the flame reflects equilibrium. Going from low to high momentum (left to right) on Fig. 4 would in general bring the diffusion flame closer to equilibrium. Higher velocities will increase strain rates resulting in more efficient mixing or shorter reaction times and hence shorter and more bluish flames.

(The main radiator for diffusion flames of interest is that due to the yellow soot particles.)

Figure 5 presents the adiabatic flame temperature calculation for the  $H_2$ -air system with liquid  $H_2O$  as an additive (NASA PROGRAM CEC-76). There are a family of curves of  $T$  vs. hydrogen mole fraction at various water to gas ratios. Consider first the uppermost curve with  $\dot{m}_{H_2O} = 0$ . For a constant 2 moles of  $H_2$  the number of moles of air is given as  $1/\phi$ . For a stoichiometric mixture,  $\phi = 1$ , one obtains the maximum temperature. For fuel rich systems,  $\phi > 1$ , insufficient  $O_2$  is present in order to burn all the  $H_2$  so the temperature falls. In fuel lean cases,  $\phi < 1$ , there is an excess of  $O_2$  being carried along but not participating in the reaction and hence temperature falls. The <sup>excess</sup> $O_2$  acts as a diluent, it has to be raised to the final temperature without contributing anything to the heat release process (see Eq. (8)). These concepts work well with a premixed flame where  $\phi$  can be set by mixing in the appropriate proportions. In a diffusion flame, on the other hand, where the oxidant is mixed into the fuel jet via entrainment of the surrounding air,  $\phi$  will vary throughout the height of the flame, very large near the burner exit and falling as the mass of entrained air increases with height.

The remaining curves on Fig. 5 show the effect of various ratios of liquid water to hydrogen,  $\dot{m}_{H_2O}/\dot{m}_{H_2}$ . In general, the shapes resemble the no-water case with, as expected, lower temperature levels a function of increased water flow rates. For a given  $\phi$  the curves shift slightly to the left with increased water due to the larger denominator of the abscissa. The thermodynamic advantage of liquid water (l) vs. steam (v) is seen by two examples

showing vertical lines between v and l. (The calculation is obviously not concerned about how one gets the liquid into the mixture.)

The idea of a limit flame temperature below which extinction results has been a successful one for certain simple geometries. Ishizuka and Tsuji<sup>12</sup>, for example, have studied counterflow laminar diffusion flames at the stagnation point of a porous cyclinder. By independently varying the amount of inert gas in both the fuel and oxidizer streams, limiting values of fuel and oxygen as well as the corresponding measured flame temperatures at those limits were obtained. The flame temperature at the two concentration limits nearly coincide and come close to the flame temperature at the lean flammability limit of a premixed system. The quoted figures<sup>12</sup> for  $\text{CH}_4$  and  $\text{H}_2$  were 1473 K and 1013 K, respectively, both using nitrogen as diluent. (For hydrogen the limit mole fraction for  $\text{H}_2$  in "normal" air determined was .114 and for pure fuel the limit mole fraction for  $\text{O}_2$  was 0.052. The corresponding numbers for  $\text{CH}_4$  were 0.165 and 0.143.)

If this concept of extinction as a limit temperature was valid in general all that would be required would be for one to go to a calculation like Fig. 5 for the particular fuel of interest and find the amount of water which for all  $\phi$  would keep the flame temperature below that predetermined extinction limit temperature.

The decrease in temperature due to liquid water,  $\Delta T_{D-W}$  (dry-wet), as a function of the mole fraction of water in the reactants can be seen explicitly in Fig. 6 for hydrogen and acetylene, two fuels representing the extremes of sooting or radiative characteristics. Note these are for a single mixture

ratio, namely, stoichiometric,  $\phi = 1$ . One can observe the distortion between the mass ratios and the mole fraction for  $H_2$  due to its molecular weight.

### 3.2 Flame Stabilization

Peters and Williams<sup>13</sup> have recently studied the structure of lifted turbulent diffusion flames at exit velocities between liftoff and blowoff values. They show that molecular mixing time may not be of sufficient duration to view stabilization as the equality of local flow velocity with a premixed turbulent burning velocity, as conventionally viewed. Here blowoff would occur when the exit velocity was sufficiently high (and the base of the flame sufficiently far from the exit) such that the mixture composition reached a fuel lean limit everywhere across the jet. Instead, they propose a mechanism involving sufficient scalar dissipation or strain rate such that the distorted laminar diffusion flamelets composing the flame are stretched excessively to the point of quenching. Reasonable agreement between the analysis and liftoff heights of  $CH_4$  jet diffusion flames is demonstrated.

Kalghatgi<sup>3</sup>, on the other hand, has correlated a huge amount of blowoff data using the former interpretation of stabilization or extinction. The expression for non-dimensional blowoff velocity,  $\bar{U}_e$ , vs. flame Reynolds number,  $R_H$ , based on a lift off distance,  $H$ , where fuel concentration has fallen to a stoichiometric mixture, is:

$$\bar{U}_e = 0.017 R_H (1 - 3.5 \times 10^{-6} R_H) \quad (3)$$

where

$$\bar{U}_e = \frac{U_e}{S_u} \left( \frac{\rho_e}{\rho_\infty} \right)^{1.5} \quad \text{and} \quad R_H = \frac{H}{v_e} \frac{S_u}{v_e}$$

$$H = \left[ 4 \frac{\bar{\theta}_e}{\bar{\theta}_s} \left( \frac{\rho_e}{\rho_\infty} \right)^{1/2} + 5.8 \right] d_e \quad \text{from cold jet measurements}$$

and

$U_e$  - exit velocity at blowoff

$S_u$  - maximum laminar burning velocity of the fuel with the ambient

$v_e$  - kinematic viscosity of fuel gas

$\rho_e$  - density of fuel at burner exit

$\rho_\infty$  - ambient density

$\bar{\theta}_e$  - fuel mass fraction at burner exit

$\bar{\theta}_s$  - fuel mass fraction in a stoichiometric mixture with the ambient

$d_e$  - effective burner diameter =  $d_b$ , actual diameter for subsonic jets

$$d_e = d_b \left[ \frac{2 + (\gamma-1)M^2}{\gamma + 1} \right]^{\frac{\gamma+1}{4(\gamma-1)}} M^{-1/2}$$

$\gamma$  - ratio of specific heats

$M$  - Mach number

It is apparent that the blowoff velocity depends almost linearly on diameter and on  $S_u$  to the second power, besides depending on the other thermochemical and physical properties of the fuel. The value of the above correlation here, is that it works for mixtures (see Fig. 1, the  $\text{CO}_2/\text{C}_3\text{H}_8$  results obey the correlation reasonably well) provided that the effect of the diluent

on the above parameters are accounted for. In particular the parameters  $S_u$  and  $v_e$ , require some further estimations for their determination as opposed to a straight mole fraction conversion. But conceptually, Eq. (3) ought to allow one to calculate the reduced blowoff velocity due to water droplet ingestion from a purely "premixed" extinction point of view. That is to say, the results must be tempered by the fact that the drops, beside needing a finite evaporation time or distance, are coming into the gas jet in the mixing region and are not being premixed as steam (Eq. (3) is applicable only to diluent gases) upstream of the burner exit. It will be interesting to compare these results with an equilibrium calculation in light of the idea of a limit temperature (at blowoff) seemingly successful in the counterflow-stagnation point diffusion flames discussed previously.

### 3.3 Momentum and Droplet Characterization

The application of an explosive charge set near actual blowout fires, presumably resulting in a pressure wave of such magnitude as to separate the flame from the pipe or other "holding" structure, has apparently been used successfully in previous blowout fire extinguishment. This, then, would be utilizing a mechanism not previously discussed explicitly under thermodynamics or flame stabilization in the normal sense of simple blowoff. Some of the features of this kind of mechanism are discussed below.

(a) Kalghatgi's Effect of Cross Wind. Kalghatgi in Part II of Ref. 3 has studied the effect of cross wind on the blowoff stability of small diameter jet diffusion flames. For a variety of common gases he determined a universal non-dimensional stability curve - a plot of jet velocity,  $U_e$ , at blowoff

versus crosswind velocity,  $V_\infty$ , separating stable flames from those blown off by the crosswind. The characteristic velocity for both  $U_e$  and  $V_\infty$  making the curve non-dimensional and applicable to all the gases is

$$W = S_u \left( \frac{HS_u}{v_e} \right) \left( \frac{\rho_e}{\rho_\infty} \right)^{-1.5} \quad (4)$$

The analogy with stabilization of flames without cross wind is clear, i.e., the same parameters as those used in the Eq. (3) correlation.

For a single gas-burner combination there is a limiting value of  $V_\infty$  beyond which a stable flame is not possible, i.e., blowoff results for any  $U_e$ . Below this critical value of  $V_\infty$  there exists two values of  $U_e$ , a high and low value, which define the stability envelope. From the universal plot (Kalghatgi<sup>3</sup>, Part II, Fig. 6) the critical value of  $V_\infty$  is about  $V_\infty/W \sim 0.6 \times 10^{-3}$  for  $U_e/W \sim 12 \times 10^{-3}$ . The relative momentum of the wind to the jet at blowout, then, can be estimated as:

$$\frac{\rho_\infty V_\infty^2}{\rho_e U_e^2} \sim 0.0025 \frac{\rho_\infty}{\rho_e} \quad (5)$$

with  $V_\infty/U_e$  equal to about 0.05. For  $V_\infty$  less than critical the lower stability curve yields values of relative momentum much higher than the value at criticality. These, however, are generally flames of much lower burner Froude number than those one would expect to encounter in the present study. The upper portion of the stability curve below criticality will yield momentum ratios lower than Eq. (5).

It would appear then from equation (5) that a not unreasonable amount of perpendicularly directed momentum could be responsible for flame instability. Although for large values of  $U_e$ ,  $V_\infty$  will not be trivial. Judgement should be tempered, however, for any extrapolation to large diameter flames since those flames forming the stability curve were from diameters below the critical choked diameter as dictated by the Annushkin and Sverdlov<sup>10</sup> analysis or the Kalghatgi<sup>3</sup> extrapolation contained in Table 2.

(b) Droplet Dynamics. It is conceptually simple to write mass, momentum and energy balances on a single droplet particle entering a flowing hot stream. For example Fig. 7 shows the first stage of a droplet injection model involving simple momentum conservation between a nonevaporating particle and a flowing gas stream. The figure shows the trajectory,  $y^*(t^*)$  vs.  $x^*(t^*)$ , of a single particle injected horizontally at  $x^* = y^* = 0$  with initial velocity,  $V_o$  into a perpendicularly flowing gas stream. The parameter is the ratio of the gas velocity to the particle velocity,  $V_g/V_o$ . Shown on the figure by hatch marks is the corresponding time,  $t^*$ .

$$x^* = \frac{x}{D_p} ; y^* = \frac{y}{D_p} ; t^* = \frac{tV_o}{D_p}$$

where  $D_p$  is the particle diameter. For example, if  $D_p = 1$  mm then  $x^* = 100$  corresponds to a distance of 10 cm, a not unreasonable thickness for the gas stream. For  $V_g/V_o$  around 10 to 20 the particle would more than likely be lost, i.e., go through the gas stream. For those streams with ratios close to  $V_g/V_o = 100$  the particles would be effective in staying in the gas stream. The model contains buoyancy forces and the effect of the density ratio which is significant and is illustrated by the dashed lines corresponding to

$V_g/V_o = 20$ . By increasing the density ratio we can easily match the performance of a particle in a higher velocity ratio stream which has lower gas density. Besides the two parameters shown in figure 7, the model allows the initial injection angle to vary and also is flexible regarding a drag model and buoyancy effects.

The next stage of the model would involve an energy balance around the particle with some evaporation mechanism. See, for example, those used in Ref. 14 through 17. Additionally the problem is not about the behavior of a single drop but the interaction of many drops in a spray, and generally not of a single size but rather a distribution of droplet sizes and, perhaps also, a distribution of initial particle velocities. Atomization from different nozzle configurations is reviewed in Ref. 18 and size distribution results for PAN types are found in Ref. 19.

In figure 7 it is assumed that the single particle did not disturb the uniform field of the gas jet. In reality a spray of particles will significantly disturb the flow field at the exit of the spray nozzle. Momentum exchange will induce a velocity in the surrounding environment of the nozzle. Due to the large density difference this entrained velocity is not trivial and this principal is actually used in practical pumping devices. Examples of the good agreement between a simple momentum balance calculation and measured entrained gas flow rates are contained in Ref. 20 and 5.

(c) The Grand Model. In the above discussions about the dynamics of particles it has been assumed that the particles are interacting with a hot, inert flowing gas - there was no mention of the effects that the evaporating

particles might have on the combustion process or flame stability. It is conceivable that a set of equations or model of the entire phenomenon could be proposed and perhaps, even solved. These would include, among others, all the coupled conservation equations for particles as well as the fuel/air including radiative and turbulence effects and the entire chemical kinetics of the combustion process. Mitani<sup>21</sup> has recently applied this approach to the effects of inert dusts and sprays on flame inhibition through premixed gases. There is considerable work required, however, to take these results and answer practical inhibiting questions even in premixed situations.

It is implicit in the discussion so far that this approach has not been taken here. Although intimately coupled the mechanisms have been looked upon as being isolated and independent. Each of the pieces of an overall model is technically difficult - the complete characterization of turbulent diffusion flames even without inhibiting sprays constitutes a large research effort involving many active participants in various laboratories around the world. Combining a series of poorly understood processes together will obviously not increase confidence in the results. Eventually all the pieces will be put together in a grand scheme, hopefully, when the physics and chemistry of all the processes are better understood.

#### 4. EXPERIMENTAL RESULTS

##### 4.1 Pneumatic Atomizing Nozzles

The spray nozzles chosen for detailed measurements are called pneumatic atomizing nozzles (PAN) or twin fluid nozzles and are used extensively in

industry for humidification purposes since the resulting drop size are usually smaller than purely hydraulic nozzles. The latter depend only upon the fluid pressure to break up the drops. Generally, for the former, the liquid exits from a central orifice or tube and is broken up by a high velocity jet of air emerging from a concentric annulus. Figure 8 shows a schematic of a typical PAN. For detailed measurements it is desired to know precisely the amount and characteristics of the spray entering the flame. This can be accomplished by using the flame gas of interest to breakup the water in place of the normally used air. The concentric annulus becomes the burner exit and in the absence of water will provide a fully turbulent jet diffusion flame when the pressure of the gas is high enough for the nozzle to work effectively. When water is admitted all the drops become intimately mixed with the fuel gas. For the present, small scale results the nozzles are used as is; in larger scales the PAN can be mounted within a pipe (Fig. 8) which can carry the bulk of the flame gas. A small portion of the gas would be used directly in the nozzle for water breakup purposes.

The gases used in the initial phase were commercial hydrogen and acetylene, both of which have sufficient stability to flame blowout at the range of pressures required for operating the small diameter nozzle.  $H_2$  with virtually no soot can be used to characterize the flame at the high momentum limit.  $C_2H_2$  would certainly represent the most luminous hydrocarbon expected in the real situation. The two can be mixed in proportion to any desired luminosity or soot level expected.

The nozzle was a Spraying Systems Co.\* 1/4 JH air atomizing nozzle with measured diameters of 0.48 mm ID for the water tube and 1.77 mm and 1.30 mm for the outer and inner annular diameters, respectively.

#### 4.2 Centerline Temperature

Figure 9 shows mean centerline temperature measurements as a function of height above the nozzle,  $z$ , both without water and with water spray for a typical  $H_2$  flame. Two types of thermocouples were used in obtaining this and subsequent data: 250  $\mu$  type K (chromel vs. alumel) above the flame tip and 500  $\mu$  type B (platinum 6% rhodium vs. platinum 30% rhodium) in the flame. The reason for the large size wire and exotic alloy in the flame is that smaller and less exotic wire simply melt due to the very high temperatures. These are very high velocity, very efficient flames in the high momentum limit. For example, a 127  $\mu$  platinum vs. platinum 10% rhodium thermocouple melts and beads up immediately upon insertion into the flame area. The temperature measurements on Fig. 9 have not been corrected for radiation. Since most of the analysis to follow is concerned with temperature differences due to water injection it is assumed that any radiation correction or catalytic effects upon the measurement will be similar in the two cases. Also the measurements were not extended all the way down to the burner exit since the question of direct impingement of droplets on the thermocouple would be raised. Also one avoids the bimodal temperature profiles by keeping away from the exit. Further clarification of this point will follow in the discussion on scaling of the flames.

---

\*Implies no endorsement by NBS.

The effect of water droplets is clearly indicated on Fig. 9. Starting with a temperature difference in the order of 300 K in the flame region the difference slowly decreases as one proceeds higher into the flame plume. Shown on Fig. 9 for reference is the solid line representing corrected centerline temperature data from Kent and Bilger<sup>22</sup>. Although the two flame conditions are not exactly the same - the Kent/Bilger<sup>22</sup> experiment utilized a coflowing air stream of velocity a tenth of the H<sub>2</sub> jet, and although turbulent, the flame had an exit Froude number an order of magnitude lower than the present results - the profile as seen on Fig. 9 and the temperature levels are similar. Also shown on the solid curve are some centerline concentration measurements, for H<sub>2</sub>:1%, and O<sub>2</sub>:0.5% and the location of a centerline stoichiometric mixture,  $\phi = 1$ , as given by Kent and Bilger<sup>22</sup>. Shown also on Fig. 9 is a hypothetical  $\phi$  profile calculated from equilibrium for the dry case using measured temperatures. For low  $z$  values the rich side of Fig. 5 is used up to the maximum temperature after which the lean side is used as  $z$  increases.

#### 4.3 Scaling the High Momentum Limit

Since the pneumatic atomizing nozzle appears to be an effective laboratory tool for studying the effect of droplets on turbulent jet diffusion flames near the high momentum limit (constant flame height) it was desired to carefully characterize these flames for future reference. Fig. 10 presents centerline data vs. height above the burner for various flow rates of pure H<sub>2</sub>, an excellent candidate since it avoids the soot formation process. Other fuels can be related, albeit approximately, back to H<sub>2</sub> in terms of  $\chi$ , the particular radiative fraction of the flame at the conditions of interest. By

study of individual centerline data such as that shown on Fig. 9 one can obtain the scaling parameters seen on Fig. 10. The ordinate is  $\Delta T/T_0 \times Q$  where  $\Delta T = T - T_0$  (K),  $T_0$  is the ambient temperature, and  $Q$  is the net calorific potential of the fuel. The abscissa is  $z/Q$ ,  $z$  is the height above the nozzle exit. Through a factor of about four in heat release rate all the data for different flames scale or fall on the same straight lines.

The flame is divided into three regimes. Starting high above the flame is the buoyant plume with the characteristic temperature difference dependence of  $-5/3$  power with height. Lower down is an intermediate regime where temperature dependence is weaker with height, i.e.,  $-5/4$  power. Finally, near the flame tip and in the flame itself, termed the flame jet region, the dependence on  $z$  is more complex but the flames are independent of heat release rate,  $Q$ . The dependence on  $Q$  decreases as the flame is approached: in the plume  $\Delta T \sim Q^{2/3}$  while in the intermediate region  $\Delta T \sim Q^{1/4}$  and finally in the flame jet  $\Delta T \sim Q^0$ . This is consistent with the concept of a high momentum limit (see discussion on Froude number) i.e., flame height independent of  $Q$ . With increased flow the radiative fraction falls with better jet mixing but for  $H_2$  this is of little consequence since that number is relatively small to begin with (see measurements for  $H_2$  PAN on Fig. 4).

In the flame jet regime the height dependence of  $\Delta T$  can be crudely divided into a constant maximum temperature area followed by a  $z^{-1}$  dependence up to the intermediate regime where the  $z$  dependence becomes stronger,  $-5/4$  and stronger again in the plume,  $-5/3$ . Recall that data much below the maximum temperature is not of interest at the moment due to possible direct impingement of water droplets on the thermocouple when the spray is used. One

obviously sees the decreasing temperature levels on Fig. 10 (or 9) at  $z$  less than the location of the maximum temperature. The derived scaling parameters on Fig. 10 automatically separate the flame jet data according to heat release rate.

The horizontal or maximum temperature lines are for a  $\Delta T = 1655 \pm 50$  K. There is, in truth, a slightly increasing temperature dependence on heat release rate here (100 K for a factor of 4 times in  $Q$ ) but for characterization purposes this can be ignored consistent with the constant flame height limit. The maximum temperature line remains constant out to a position of about 0.65 the height of the flame after which temperature begins to fall with  $z^{-1}$ . There ought to be a lower limit on  $Q$  or  $U$  where this correlation will not work. At low enough  $Q$  or Froude number, flame height will begin to depend on  $Q$  or the flame could actually become laminar. The other lines on the figure are least squares fit to the data in each regime along with the numerical value of the fits.

It is interesting to compare the derived scaling of Fig. 10 with studies involving non-combusting vertical buoyant jets in uniform environments. Chen and Rodi<sup>23</sup> have reviewed the literature and correlated a lot of data for buoyant jets. In particular, their Fig. 5, p27 showing centerline decay of density in axisymmetric buoyant jets is remarkably similar to the flame temperature data on Fig. 10. There are three regimes, the non-buoyant region being independent of initial densimetric Froude number analogous to the present flame jet region independent of  $Q$ . The  $-1$ ,  $-5/4$  and  $-5/3$   $z$  dependence respectively in the three regimes is identical to the present Fig. 10. The correlations of Chen and Rodi<sup>23</sup> are, guided by certain scaling laws, made non-

dimensional in terms of reference density, source Froude number, exit diameter, etc. For the present, Fig. 10 is left in terms of the minimum number of primitive variables which were actually varied until more is learned of the behavior of jet flames.

#### 4.4 Effect of Spray

Besides providing a "model" of high momentum jet flames, Fig. 10 will be used as a baseline to compare the effect of the water sprays on the flames. Fig. 11 shows the centerline temperature rise ( $T-T_o$ ) vs. height for a hydrogen flame with various mass flow rates of water. The coordinates and scales are identical to Fig. 10 except for heat release rate. Here an equivalent heat release rate,  $Q_E$  which equals the normal heat release rate of the flame,  $Q$ , minus the calculated cooling effect of water,  $Q_{H_2O}$ ,

$$Q_E = Q - Q_{H_2O}$$

Assuming an initial water temperature of 20°C the latent and specific heats comprising  $Q_{H_2O}$  are as follows:

$$\text{liquid: } 0.0042\text{kW}/(\text{g s}^{-1} \text{ K}) \times 80 \text{ K}$$

$$\text{vaporization: } 2.26\text{kW}/(\text{g s}^{-1})$$

$$\text{steam: } 0.0024\text{kW}/(\text{g s}^{-1} \text{ K}) \times (T_f - 373)$$

$$\text{or, } Q_{H_2O} \text{ (kW)} = [1.7 + .0024 T_f(\text{K})] \dot{m}_{H_2O}(\text{g/s}) \quad (6)$$

Note that for a representative flame temperature of  $T_f = 1500$  K the breakdown of the cooling capacity between the liquid plus vaporization and the steam is about 50% each. That is, the cooling capacity is doubled by the use of liquid water as opposed to steam. For the steam a constant specific heat is used for simplicity. The value chosen is for a temperature of about 1150 K midrange of the  $C_p$  value at boiling (0.0020) and that at about the expected extreme of 2000 K (0.0028).  $T_f$  is the "flame" or maximum temperature measured, corresponding to the horizontal lines on Fig. 10 and 11 or the value around  $z = 0.12$  m on Fig. 9. The calculation of the horizontal line for the case of the flame with water spray, i.e., Fig. 11, will be discussed shortly.  $T_f$  is here, obviously, a function of water flow rate.

Comparison of the data on Fig. 11 with Fig. 10 indicates that, above the flame region, the centerline temperature appears to be the same as the temperature above a flame without water but with a reduced heat release rate. The same scaling embodied in the least squares fit of the data on Fig. 10 is used for Fig. 11. The numerical values of the least squares correlation are shown on the figure. In the plume 0.093 can be compared to the dry case of .0951, similarly 0.318 vs. 0.346 in the intermediate regime, etc. So, to a first approximation, the regions above a flame cooled with water spray can be viewed as resulting from a non-sprayed flame with scaling dependent on a diminished heat release rate. The same characteristics and overall behavior is noted in the two plots, Fig. 11 and 10. This will be important later for large scale flames in evaluating the cooling effects of the spray. There is a direct correspondence between what one observes high above the flame reflected in centerline temperature measurements and what one has done to the flame below in terms of amounts of water sprayed.

Reiterating on the effect of spray - to a first approximation, we are getting the full flame exothermicity ( $Q$ ) since the flow rate of  $H_2$  into the burner is the same whether it is the dry or wet case. To those thermocouples sitting high above the flame, however, it appears that  $Q$  has been reduced since the gases flowing past them are now at a somewhat lower temperature. If the water is heated, boiled, and <sup>the</sup> steam heated, all below those thermocouples then it would appear to them that the gases flowing by are from a reduced heat source namely,  $Q_E = Q - Q_{H_2O}$ . If all the convective energy were captured at some point high above the flame one ought to be able to reconcile any differences between the wet and dry cases. The difference between the higher temperature, smaller mass flow, dry case and the lower temperature, larger mass flow (the diluent water vapor), wet case ought to equal the latent heat of vaporization of the water provided the spray has not markedly affected the entrainment process. This will be so only for the case of hydrogen since radiation is a tiny fraction of the heat release and we are ignoring any radiative changes due to the water spray. (Visibly the emission appears to increase from the dry to the wet case. This is thought due to sodium emission from water impurities<sup>24</sup>. Using a broad band radiometer the emission, in fact, decreases slightly for the wet case as expected.) For typical hydrocarbons the simple convective balance seen for  $H_2$  will be more complicated due to significant amounts of radiation and radiation reduction due to the spray (Fig. 2).

For locations actually in the flame regions the situation is much more complex than the above simple picture of temperatures, high above the flame, simply depending on an effective heat release rate. Additionally one requires to know  $T_f$  in order to calculate  $Q_E$  or  $Q_{H_2O}$ .

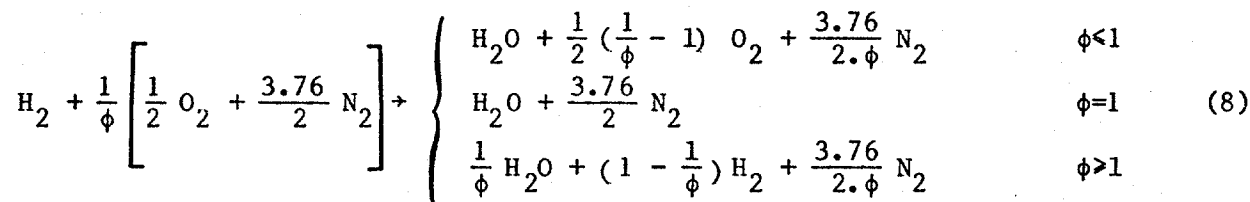
#### 4.5 Equilibrium Heat of Reaction Calculation

How the series of data on Fig. 11 reflects or mirrors equilibrium calculations can be observed on Fig. 12 which shows the normalized reduced heat release rate,  $Q_E/Q$  plotted against the water to gas ratio. For the data points,  $Q$  is the nominal heat release rate shown on Fig. 11 for the particular symbols and  $Q_E$  is calculated from Eq. (6) using measured  $T_f$  (to be discussed) i.e.,  $Q_E$  is the value used to collapse the data on Fig. 11. The equilibrium calculation requires a bit more explanation.

When a chemical reaction takes place the heat evolved (or captured) is related to the change in the enthalpy of the products (P) and reactants (R). A convenient form for this calculation is:

$$-\Delta H_{\text{COMB}} = \sum_P n_P (\Delta H_f^O)_{P,298} - \sum_R n_R (\Delta H_f^O)_{R,298} \quad (7)$$

where  $n$  is the number of moles and  $\Delta H_f^O$  is the heat of formation of the molecule conveniently tabulated at some standard state (298K). For example, the idealized reaction of  $H_2$  with air,



yields 1 mole of  $H_2O$  per mole of  $H_2$  consumed with  $\phi = 1$ . Solving Eq. (7) gives:  $-\Delta H_{\text{COMB}} = 1 \times (\Delta H_f^O)_{H_2O,298} = -57.798 \text{ kcal/mole } H_2$  since the heats of formation of  $O_2$ ,  $N_2$ , and  $H_2$  are all zero. This number, 57.798 kcal/mole, is the value contained in engineering tables as the lower ( $H_2O$  vapor) or net heat

of combustion (120 MJ/kg) and what in this report has been referred to as the net calorific potential of the fuel or nominal heat release rate or, simply, Q. Due to the dissociation of molecules at high temperatures a proper equilibrium calculation would yield a host of other species besides the  $N_2$  and  $H_2O$ . For example, the  $H_2$ -air reaction at stoichiometry ( $\phi=1$ ) yields besides  $H_2O$ ,  $N_2$ ,  $O_2$  and  $H_2$  the additional products OH, NO, H and O (neglecting others with mole fractions less than  $0.5 \times 10^{-5}$ ) all having positive values for heats of formation which tends to diminish the above negative value for  $H_2O$ . Additionally, and more importantly, in forming these species the 1 mole of  $H_2O$  created in the idealized reaction becomes something less than 1 mole: e.g., 0.942 moles for the  $\phi = 1$  example. The two effects combined result in a heat of reaction of 53.72 kcal/mole, lower than the nominal value of 57.798.

For  $\phi > 1$  there simply is not enough oxygen around to create 1 mole of  $H_2O$  and hence the heat of reaction drops dramatically. For example, the  $\phi = 1.5$  calculation yields 0.66 product moles of  $H_2O$  and a heat of reaction equal to 38.1 kcal/mole. (For  $\phi > 1$ , to a first approximation,  $n_{H_2O} \times 57.798$  kcal/mole equals the heat of reaction.) On the other hand for  $\phi < 1$  there is an ample supply of  $O_2$  available to form very close to 1 mole of  $H_2O$ . In fact in the limit of  $\phi \rightarrow 0$  one obtains the nominal value of 57.798 kcal/mole. Even though  $O_2$  will be present in large concentrations in the products and be responsible for decreased temperature as seen on Fig. 5 since it acts as a diluent (like  $H_2$  in the fuel rich case) it does not enter the calculation of heat release rate since its heat of formation is zero.

For a fixed  $\phi$  when water is added the temperature drops as illustrated in Fig. 5. The calculation for heat of reaction, Eq. 7, now contains a non-zero term for the reactants,  $n_{H_2O(L)} \times (-68.317)$  kcal, for the liquid water.

However, as far as the formation of water from the  $H_2$  and  $O_2$  is concerned the reactant water has little effect - it is simply carried along as a diluent. Instead of approaching a value of one mole of water in the products for the dry case a value close to  $n+1$  is realized, where  $n$  is the number of moles of liquid water in the reactants. The lower temperature obviously does result in less dissociation and hence slightly higher values of product water but as far as the heat of reaction calculation is concerned the only significant difference between the dry and wet case is the heat of vaporization.

This is not very useful for the present purposes. What is of interest here is a calculation that actually reflects the effect the water has on an otherwise undisturbed flame - it is desired to reference things to the flame without water, i.e., the sensible temperature change due to water must be included. This can be done in either of two ways. One involves Eq. (6) for the cooling effect of the water,  $Q_{H_2O}$ , knowing the final temperature  $T_f$  from the equilibrium calculation. The second involves knowing the two temperatures,  $T_f$  wet and  $T_f$  dry, taking the difference and multiplying by an approximate specific heat and mass of products, both also available from the equilibrium calculation. This then is what is referred to as  $Q_{H_2O}$  and  $Q_E = Q - Q_{H_2O}$  where  $Q$  is the actual heat of reaction discussed above for the solid lines representing the equilibrium calculation on Fig. 12. Two effects influence the relative positions of the lines on the figure. For small  $\phi$ ,  $T_f$  is small making  $Q_{H_2O}$  small and at the same time  $Q$  is large. Similarly for large  $\phi$ ,  $T_f$  is high and  $Q$  is low.

Comparing a jet diffusion flame to an equilibrium calculation may prove to be useful in later analysis. For now the data from Fig. 11 appear to

follow the trend of the equilibrium lines on Fig. 12 quite well. Recall that there is a factor of 2-1/2 times variation in heat release rate and water to gas ratios up to 6.6 for the data shown. It is not clear at this point why the points fall on an equilibrium calculation at a value of  $\phi$  somewhat less than 0.75, a fuel lean condition. Since the flame region is independent of  $Q$  one might speculate about the effect of the water or reduced  $Q$  being seen in the regions above the flame where a fuel lean condition exists.

Besides the ten points representing the conditions for the data on Fig. 11 there are three additional points represented by filled symbols on Fig. 12. For these data the flames were extinguished. What generally happens is illustrated by considering the 18.2 kW series. From Fig. 11 at a water to gas ratio of 3.2 there resulted a suppressed flame. Presumably with more water more suppression results, reflected in decreased  $Q_E$ . At a ratio of about 4.3 (Fig. 12) however the flame went out. Similarly for the 13.7 kW case two ratios, 1.8 and 3.7 are shown on Fig. 11. When the ratio was increased to 9.2 the flame went out. For the intermediate case of 15.6 kW the resulting ratio at extinguishment fell between the 18.2 and 13.7 kW cases. Observing where these extinguishment points fall relative to the data from simply suppressed flames is another reason for constructing Fig. 12. Nothing on that figure, however, appears to reveal information as to why those particular flames went out.

Along with the symbols on Fig. 12 the pressure of the gas for those data is given. It is clear that the higher the gas pressure (or flow reflected in  $Q$ ) the easier, in terms of either water to gas flow ratio or the absolute amount of water, it is to extinguish the flame. (Recall the discussion about

Fig. 1 which also contains this data.) In fact, under about 10 psig (9.9 to include the 13.7 kW case) the flames cannot be extinguished by any reasonable amount of water. Observe the 10.9 kW series on Fig. 11. It was apparent back on Fig. 2 that reduced radiation levels could be increased by increasing the pressure of the water in the purely hydraulic type of nozzle. A characteristic of PAN types is that the drop size will decrease with increased pressure of the gas which is breaking up the drops. A tentative explanation for both the reduced radiation on Fig. 2 and the extinguished flames on Fig. 12 could involve smaller drop sized particles being more effective in getting into and affecting the reaction zone. However, there is still not enough evidence to confirm this effect or to completely eliminate other possibilities, e.g., momentum of the spray and gas will also increase with pressure. These data obviously must be pursued further.

#### 4.6 Flame Temperature Measurements

Having somewhat characterized this "model"  $H_2$  flame in the high momentum limit in terms of scaling, location of regimes, etc. on Fig. 10 and how it is effected by water sprays on Fig. 11 as reflected by  $Q_E$ , it is now possible to look in detail at the maximum or "flame" temperature reduction as a function of water spray. The measurements are temperature levels at  $z = 0.122$  m above the burner exit (see Fig. 9). Fig. 13 presents the flame temperature reduction  $\Delta T_{D-W}$  normalized by the water to gas ratio plotted against the same water to gas ratio. Recall from Fig. 6 that equilibrium dictates a near linear variation of  $\Delta T_{D-W}$  with the amount of water introduced into the reaction so a plot of the  $\Delta T_{D-W}$  divided by water flow against water flow ought to yield an almost horizontal line. How the data deviates from such a line may offer

insight into the phenomena. One further point that should be stressed when comparing the data to equilibrium is that one is comparing the temperature differences with and without water rather than the absolute levels.

Seen on Fig. 13 are a series of data points with fixed heat release rate or gas flow rate for a variably increasing water flow rate. In general, for any gas flow, as water flowrate is increased the "effectiveness" of the spray in terms of a  $\Delta T_{D-W}$  per unit water to gas flow rate ratio decreases - there is less temperature decrease from the water. Additionally, the effectiveness level, especially at small water flow rates, depends strongly on the gas flow rate or stagnation pressure of the gas. Shown by solid (almost horizontal) lines are equilibrium calculation for various  $\phi$ . The deviation from linearity between  $\Delta T_{D-W}$  and water flow rate seen in Fig. 6 gets amplified on Fig. 13. As  $\phi$  increases the value of the negative slope increases. The comparison between the data and the lines is not as simple as in the case of Fig. 12 for  $Q_E/Q$  where there is a weak dependence of  $Q_E$  on flame temperature. These are measurements in a fuel rich regime (see Fig. 9) and should therefore compare not to  $\phi$  slightly less than 0.75 as seen on Fig. 12, but some higher  $\phi$  perhaps around  $\phi = 1.5$ . In this interpretation it is assumed that the mixture distribution does not change significantly with increased gas flow since these flames all appear to scale (Fig. 10). That is, the lower Q points should not necessarily be compared to a lower  $\phi$  than the higher Q points. In other words, when the  $H_2$  velocity is increased there are not additional fuel rich areas in the flame because the amount of entrained air is increasing at the  $\lambda$  and high values of  $\Delta T/\dot{m}_{H_2O}/\dot{m}_{H_2}$  seen in the data, proportionate to Q, is simply

*same time, in proportion with the  $H_2$  velocity. The difference between the low*

*dipping lines*

a manifestation of water droplet effectiveness - the flame hasn't changed, the spray has.

The data points on Fig. 13 can all be collapsed quite accurately into a decaying exponential of the form

$$\frac{\Delta T_{D-W}}{\dot{m}_{H_2O}/\dot{m}_{H_2}} = A \exp [-Bx \dot{m}_{H_2O}/\dot{m}_{H_2}] \quad (9)$$

where A and B are simple functions of the heat release rate, Q. This has been used to find the correlated horizontal lines shown on Fig. 11 for temperature in the flame region. Also it has been used to extrapolate those series of runs where extinguishment occurred on Fig. 12. That is, the correlation answers the question - what would the temperature be just prior to extinguishment if the trend of the data continued? The actual three extinguishment points are shown on Fig. 13 by vertical lines emanating from that extrapolated temperature level. It is not evident whether any new information is contained here. One can only say that if the extrapolation were valid then a limit temperature for this H<sub>2</sub> flame might fall between 1500 and 1600 K, quite a bit higher than Ishizuka and Tsuji's<sup>12</sup> counterflow stagnation point result for H<sub>2</sub> of 1013 K. Unfortunately these values fall right in the middle of a host of other points with similar temperatures but whose flame did not extinguish. Note that the extrapolation amount could be considered significant. These flames will be studied at water/gas ratios much closer to the actual extinguishment point.

#### 4.7 Correlation with Drop Size

If the claim that both the level and decay of the data on Fig. 13 are due to different spray characteristics it ought to be possible to correlate the data with some parameter or parameters that reflect that spray characteristic. Gretzinger and Marshall<sup>19</sup> have studied pneumatic atomizing nozzles extensively and found that the mass median diameter of sprays varied significantly with the mass ratio of atomizing air to liquid atomized. The mass median diameter is that diameter above or below which 50% of the mass or volume of the spray resides and is used extensively along with a distribution spread in the aerosol or particle science area to characterize distributions of size. The correlated findings of Gretzinger and Marshall for the median diameter,  $\bar{X}_m$  for this type of nozzle is as follows:

$$\bar{X}_m = 2600 \left[ \left( \frac{M_\ell}{M_a} \right) \left( \frac{\mu_a}{G_a L} \right) \right]^{0.4} \quad (10)$$

where  $M$  is the mass rate of flow of liquid ( $\ell$ ) and air ( $a$ ), respectively, i.e., the present  $\dot{m}_{H_2O}$  and  $\dot{m}_{H_2}$ ;  $\mu_a$  is the viscosity of air ( $H_2$ );  $G_a$  mass velocity of air at nozzle outlet which here equals  $\dot{m}_{H_2}$  /annulus area;  $L$ , diameter of wetted periphery between air and liquid, taken here as the inner annulus diameter.

It should be stressed that the intent here is not to obtain absolute values of drop size but rather approximate functional relations among the variables since the conditions of the experiments here and in Ref. 19 are not identical. Fig. 14 presents the  $H_2$  flame temperature reduction divided by the water to gas ratio plotted against the Gretzinger and Marshall<sup>19</sup> median drop

size,  $\bar{X}_m$ . With the exception of a few outliers the bulk of the data appears to correlate reasonably well with the Gretzinger and Marshall<sup>19</sup> median droplet spray diameter,  $\bar{X}_m$ . The increased effectiveness of smaller drop sized particles is clear from the figure. On the ordinate of Fig. 14 is shown the various equilibrium results for a given  $\phi$  which one might judge the data to be approaching as droplet size gets smaller and smaller.

A statistical test has not been performed on the data shown on Fig. 14. Specifically, the two lowest pressure groups, the 7.3 and 8.6 kw data, might appear to be distinct from the remaining bulk of the data. The lower pressure data have been left on the figure for completeness but the lower operating range of the nozzle may have been exceeded for those flowrates. The lower the pressure <sup>u</sup>~~x~~, the smaller is the amount of water that can be atomized. The amount of water sprayed is beyond the capacity to be completely atomized and the spray will contain unatomized droplets. At the high droplet size the fall off is consistent with what may be observed visually. Especially at low gas flow rates as the amount of water is increased to larger and larger values it begins to become apparent that all the droplets are not participating in the suppression process. Droplets are seen to escape radially from the luminous zone and fall to the laboratory floor. As the amount of water is decreased and/or the H<sub>2</sub> gas flow is increased the escaping droplets are seen to disappear. Fig. 14, then, not only contains information about the relative effectiveness of different sized participating particles but also reflects something about those larger particles which escape whole. How general this behavior is must ultimately be determined.

Shown on Fig. 14 by filled symbols are the three "extinguished" points referred to in the previous two figures. Nothing on Fig. 12, nor Fig. 13, nor finally on Fig. 14 offers a clue to distinguish these points - neither reduced heat release, extrapolated temperature nor the rough guide to median drop size appears to differentiate these points from their neighboring counterparts. Recall that these points are at high  $H_2$  flow rates or pressure but not so high as to have blowout without the water drops added. They therefore contain most, if not all, of the information required for understanding the phenomena of jet diffusion flame suppression using water sprays and the unravelling of this information will provide the focal point of future efforts.

#### 5. CONCLUSIONS AND RECOMMENDATIONS FOR FUTURE STUDY

From the evidence of laboratory data by O'Neill<sup>2</sup> on large-sized flames and the other small scale feasibility data discussed in the "Previous Observation" section, it appears likely that scaling up to the full sized blowout fire will require more than a cursory understanding of the physio-chemical mechanisms which will be involved in suppressing and extinguishing high velocity jet diffusion flames by the application of water sprays. Obvious physical phenomenon like blowoff, dilution, flame stabilization and momentum, as well as the need to be cognizant of choked flow in large pipes and the accompanying difficulties regarding suppression, were reviewed in light of the observations.

Pneumatic atomizing nozzles were shown to provide a close to ideal experimental set up for studying the phenomena. During this study, soot free  $H_2$  flames were used to model the behavior of diffusion flames at the high

momentum limit of the Froude number scale. Primitive scaling parameters were obtained for future study of other fuels and scales. Effects due to the spray could be characterized away from the flame region by an effective heat release rate, a function of the amount of spray. The behavior of the "model"  $H_2$  flame was compared to thermodynamic equilibrium calculations thus establishing equilibrium as a viable tool for studying jet diffusion flames. Finally, reduced flame temperature measurements were shown to correlate with a single parameter characteristic of the water spray - the median drop diameter.

The results of this effort provide a rational starting point for future studies. For detailed characterization in the small scale, pneumatic atomizing nozzle configuration there is an excellent opportunity to pursue the actual mechanism of extinction further - the location of those three "extinguishment" points in amongst only suppressed flames have been determined. It is suggested that by approaching those points, e.g., slowly increasing the water to gas ratio from a known suppressed flame location, and observing changes in measurable quantities one can isolate this particular kind of extinguishment.

A program will shortly begin in the large laboratory regime (Table 1) utilizing more common hydrocarbons in a larger PAN configuration. These flames will be instrumented in a manner which will allow direct comparisons to the findings of the present study. Adjusting for radiative differences any effect of scale ought to begin to become apparent. Additionally, exterior spraying can begin when the PAN results are understood fully so as to apportion differences in observed variable behavior to different droplet effectiveness. Experimentation in the industrial test facility ought to proceed at

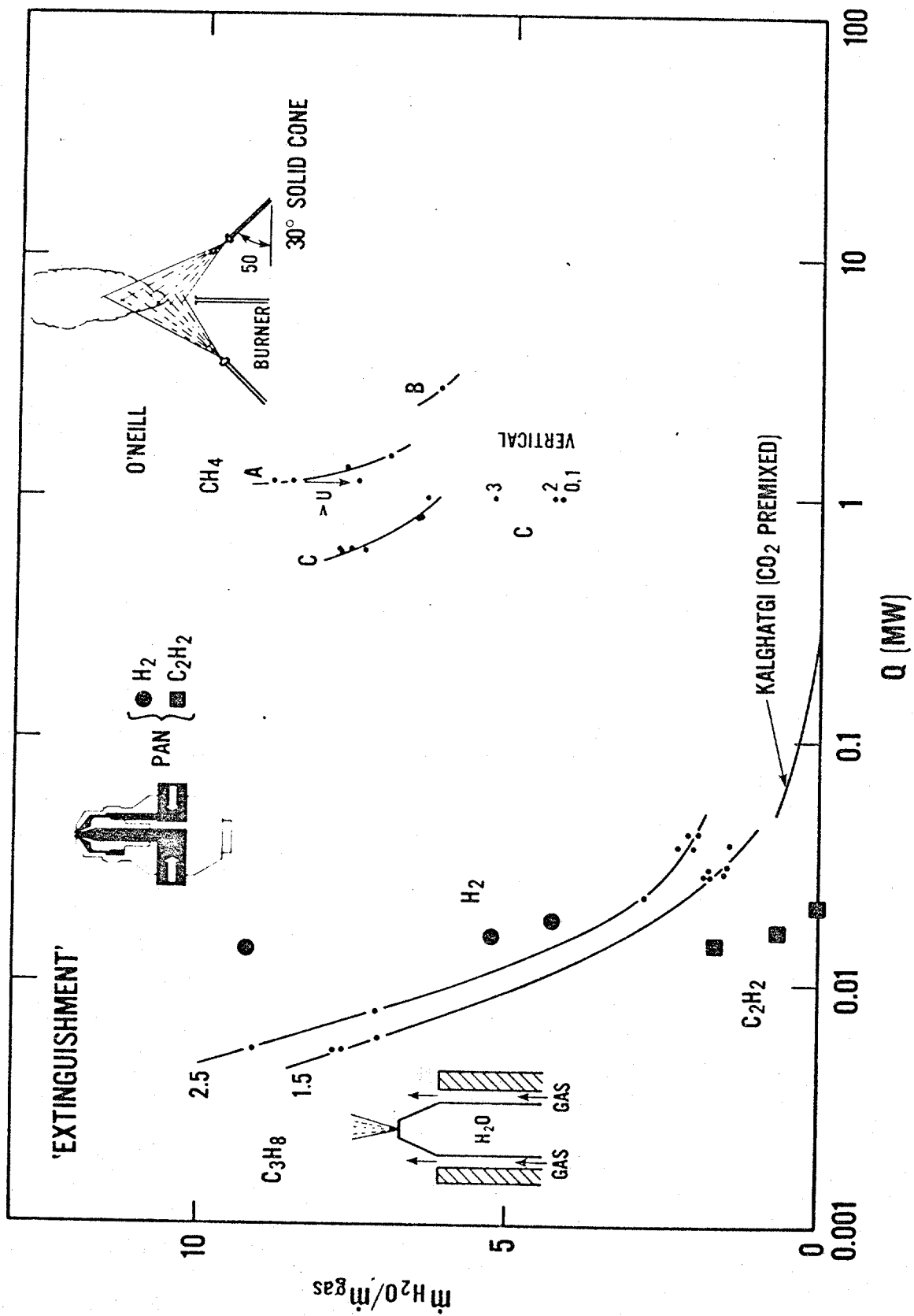
this juncture. Any noted scale effects in the smaller facility ought to become exaggerated at this level.

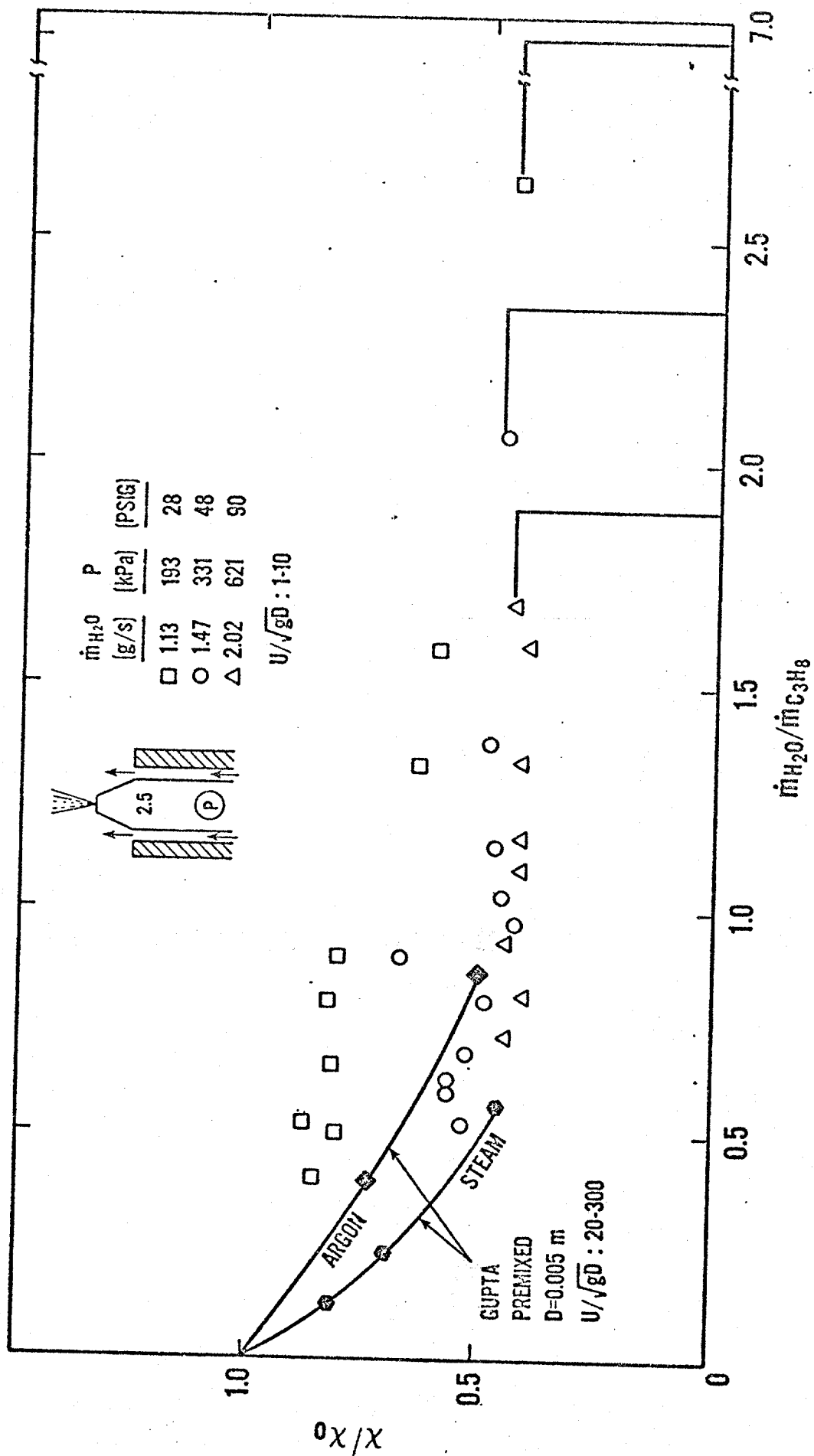
Analytical modeling of the various pieces of the problem, some of which was discussed in the report, can be performed simultaneously with the experimental work. As noted in the report, however, care should be exercised in extrapolating predicted behavior of jet diffusion flames (with or without spray) to very large scale without some experimental confirmation.

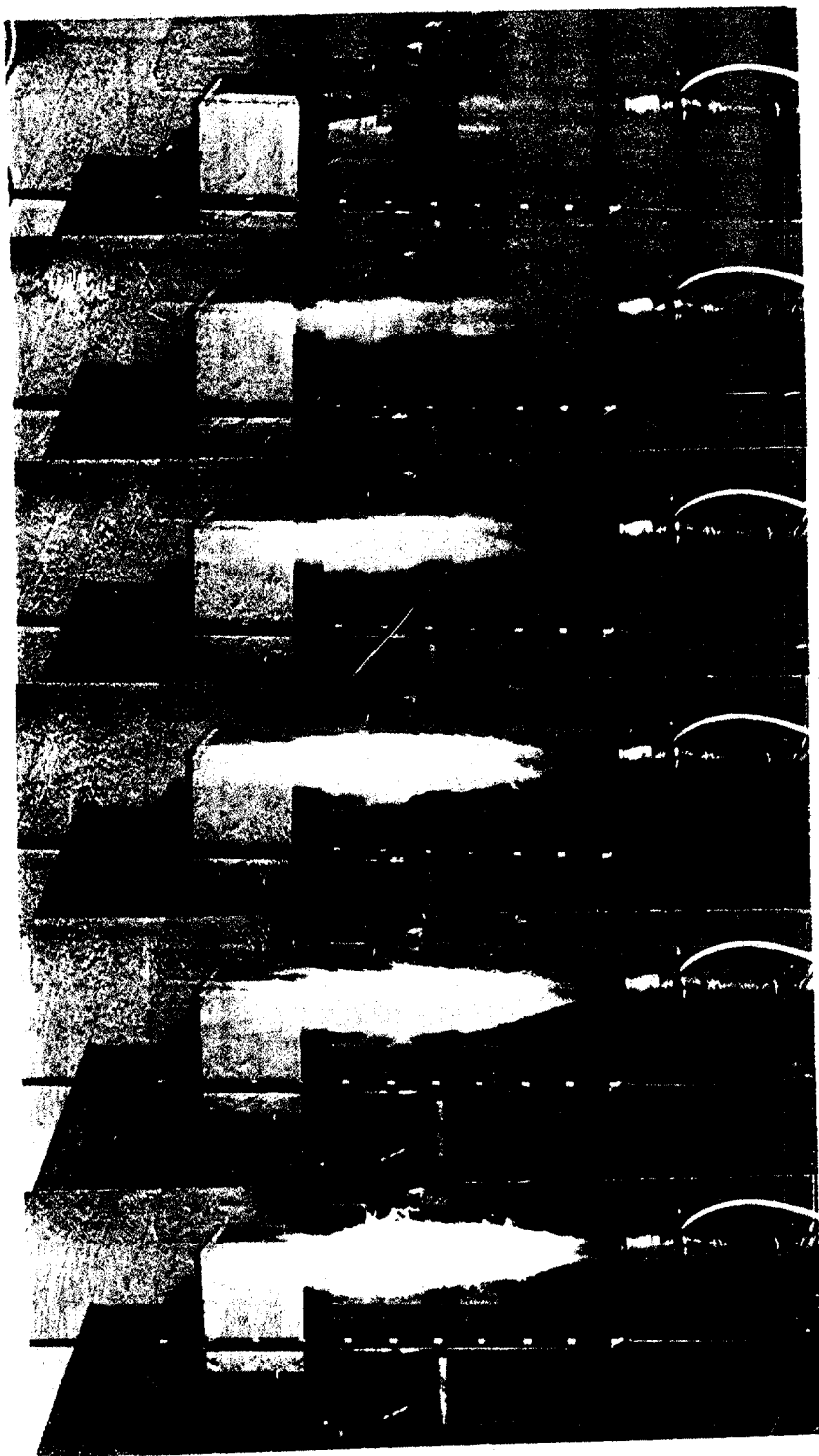
## 6. REFERENCES

1. Anon, "How a Fire Brigade Reacted to First On-Shore Oil Rig Fire", Fire 74, 587 (1982).
2. Evans, D. and O'Neill, J., Feasibility Study of Gas Well Blowout Fire Extinction, NBSIR - to be published.
3. Kalghatgi, G. T., Blow-Out Stability of Gaseous Jet Diffusion Flames, Part I: In Still Air; Part II: Effect of Cross Wind, Combustion Science and Technology 26 233 and 241 (1981).
4. McCaffrey, B. J., Some Measurements of the Radiative Power Output of Diffusion Flames, Paper No. WSS/CI 81-15, Western State Section/Combustion Institute Meeting, Pullman, Washington, April 1981.
5. Aoki, K and Matsuo, H., Development of Smokeless Flare Stack, IHI Engineering Review (Tokyo) 7 1 (1974).
6. Gupta, M. P., Experimental Investigation of the Radiation From Turbulent Hydrocarbon Diffusion Flames, M.A.S. Thesis, University of Waterloo, March 1976.
7. Becker, H. A. and Liang, D., Total Emission of Soot and Thermal Radiation by Free Turbulent Diffusion Flames, Combustion and Flame 44, 305 (1982).
8. Markstein, G. H., Scaling of Radiative Characteristics of Turbulent Diffusion Flames, Sixteenth Symposium (Int.) on Combustion, The Combustion Institute, Pittsburgh p. 1407 (1976).
9. Brzustowski, T. A., Gollahalli, S. R., Gupta, M. P., Kaptein, M and Sullivan, H. F., Radiant Heating from Flares, American Society of Mechanical Engineers, New York, Paper 75HT4 (1975).

10. Annushkin, Y. M. and Sverdlov, E. D., Stability of Submerged Diffusion Flames in Subsonic and Underexpanded Supersonic Gas-Fuel Streams, Combustion Explosion and Shock Waves 14, 597 (1979).
11. Markatos, N. C., Spalding, D. B., Tatchell, D. G. and Mace, A. C. H., Flow and Combustion in the Base-Wall Region of a Rocket Exhaust Plume, Combustion Science and Technology 28, 15 (1982).
12. Ishizuka, S. and Tsuji, H., An Experimental Study of Effect of Inert Gases on Extinction of Laminar Diffusion Flames, Eighteenth Symposium (Int.) on Combustion, The Combustion Institute, Pittsburgh p 695 (1981).
13. Peters, N. and Williams, F. A., Lift-Off Characteristics of Turbulent Jet Diffusion Flames, AIAA Paper No. \_\_\_\_\_ (1982).
14. Liu, S. T., Analytical and Experimental Study of Evaporative Cooling and Room Fire Suppression by Corridor Sprinkler System, NBSIR 77-1287, National Bureau of Standards, Washington, DC, November 1977.
15. Beyler, C. L., The Interaction of Fire and Sprinklers, NBS-GCR-78-121, National Bureau of Standards, Washington, DC, September 1977.
16. Alpert, R.L., Calculated Interaction of Sprays with Large-Scale, Buoyant Flows, ASME Winter Annual Meeting, Phoenix, Arizona, Nov. 14-19. 1982.
17. Sapko, M. J., Furno, A. L. and Kuchta, J. M., Quenching Methane-Air Ignitions With Water Sprays, Bureau of Mines Report of Investigations 8214 (1977).
18. Fraser, R. P. and Eisenklam, P., Liquid Atomization and the Drop Size of Sprays, Trans. Instn. Chem. Engrs. 343, 294 (1956).
19. Gretzinger, J and Marshall, W. R., Characteristics of Pneumatic Atomization, A.I.Ch.E. Journal 7 312 (1961).
20. Morgan, H. P. and Bullen, M. L., Smoke Extraction by Entrainment Into a Ducted Water Spray, F. R. Note 1010, Fire Research Station, Borehamwood, England (1974).
21. Mitani, T., A Flame Inhibition Theory by Inert Dust and Spray, Combustion and Flame 43, 243 (1981).
22. Kent, J. H. and Bilger, R. W., Turbulent Diffusion Flames, Fourteenth Symposium (Int.) on Combustion, p615, The Combustion Institute, Pittsburgh, PA (1973).
23. Chen, C. J. and Rodi, W., Vertical Turbulent Buoyant Jets, A Review of Experimental Data, Pergamon Press, Oxford, p27 (1980).
24. Mallard, G., private communication.







0.58

0.46

0.35

0.23

0.12

0

$\dot{m}_{H_2O} / \dot{m}_{C_3H_8}$

